PNAS
www.pnas.org

Supplementary Information for

Majority of US urban natural gas emissions unaccounted for in inventories

Maryann R. Sargent[a*], Cody Floerchinger[a], Kathryn McKain[b], John Budney[a], Elaine W. Gottlieb[a], Lucy R. Hutyra[c], Joeseph Rudek[d], and Steven C. Wofsy[a]

[a]John A. Paulson School of Engineering and Applied Sciences Harvard University, Cambridge, MA 02138

[b]Global Monitoring Division, NOAA Earth System Research Laboratory, Boulder, Colorado 80305

[c]Department of Earth and Environment, Boston University, Boston, MA 02215

[d]Environmental Defense Fund, New York, NY 10010

*Corresponding author: **Maryann Sargent**

Email: mracine@fas.harvard.edu

This PDF file includes:

Supplementary text
Figures S1 to S8
Tables S1 to S3
SI References

Supplemental Material

S1. Methane Measurement Network

Atmospheric CH_4 concentrations were measured continuously from September, 2012 to April, 2020 at two sites near the urban center and three background sites using Picarro cavity ring down spectrometers (1). Urban CH_4 measurements were obtained at Boston University (BU) and Copley Square (COP) in Boston, while background measurements were obtained at Harvard Forest in Petersham, MA (HF), Canaan, NH (CA) (maintained by Earth Networks, Inc.), and Mashpee, MA (MVY) (maintained by Earth Networks, Inc.) (Table S1). Hourly averaged concentrations were used for this analysis, with a focus on afternoon hours (11 am to 4 pm local standard time). All sites are calibrated daily, traceable to World Meteorological Organization (WMO) standards. Cross-calibration campaigns were carried out annually with a two point linear calibration across the network to ensure comparability of the measurements.

Sample air to all instruments was dried using Nafion driers beginning in July, 2013. For data obtained from September, 2012 – July 2013, empirical H_2O correction factors were used based on H_2O concentrations measured with each instrument to convert measured to dry molar fractions of CH_4. Instrument-specific H_2O correction factors were derived for the HF and COP instruments according to the methods described in (2), while correction factors from the literature (2) were applied to the BU instrument.

Total analytical uncertainty is approximated as the sum of measurement precision, uncertainty in calibration and surveillance tank values, and uncertainty in the H_2O correction. Long-term drift was not included in the calculation of total analytical uncertainty because it was captured via calibrations and corrected for in the data processing. During the first year of the experiment, when sample air was not dried, uncertainty in the H_2O correction equation is estimated as ±2 ppb at H_2O concentrations up to 3.4% (2), the maximum ambient measured H_2O concentration. During the first year, total analytical uncertainty of hourly average CH_4 measurements among the 5 sites was ≤ ~3 ppb (95% CI), < 0.2% of ambient concentrations. During the subsequent 7 years when sample air streams were dried, total analytical uncertainty of the measurement was ~1 ppb. Further details regarding network design are available in (3).

S2. Prior Flux Estimates

We produced a 1-km resolution prior model of anthropogenic and biogenic CH_4 emissions, including sources from residential and commercial NG use, pipelines, wetlands, enteric fermentation, onroad, and point sources including landfills, NG facilities, and wastewater treatment plants. Enteric fermentation and onroad CH_4 emissions were obtained from the inventory described by McKain et al. (4). Landfill emissions were based on facility-level data reported to the EPA GHG Reporting Program (GHGRP) (5), DEP (6) (7), and LMOP (8). The spatial distribution of wetland emissions was based on the McKain inventory at 1-km resolution, while a range of total emissions were compared ranging from the totals in the McKain inventory to the totals from the WetCHARTs inventory (9). While the McKain inventory had no seasonal variability in wetland emissions, WetCHARTs has significant seasonal variability with higher emissions in the growing season; we used monthly average WetCHARTs emissions, with no inter-annual variability. We tested the McKain total emissions, the WetCHARTs total emissions, 0.5*WetCHARTs total, and 0.25*WetCHARTs total, all with the spatial distribution from McKain. The results of the wetland sensitivity study are discussed in Section S4, and total wetland emissions of 0.5*WetCHARTs were used for the main results in the paper, which makes

total wetland emissions equal to the emissions from McKain et al. in the winter, and ~7X higher than the McKain emissions in the summer.

NG point source and wastewater treatment emissions were based on GHGRP data (5). Residential and commercial building losses including appliances and interior pipes were spatially distributed according to the McKain inventory, with totals for residential building losses based on (10) (11) (12) and commercial building losses based on (13). Distribution pipeline emissions were also distributed spatially according to the McKain inventory, while total emissions were calculated by combining the emission factors for different pipeline materials from Weller et al. (14), with the miles of each type of pipe in the city (15).

For the purposes of the inverse analysis and calculating top-down emissions, NG emissions – the sum of point sources, residential and commercial building losses, and pipeline losses – were scaled such that the ratio of NG:biological emissions matched that determined by the ethane:methane ratio measured in Boston. We used this approach because NG emissions from the prior inventory are not well constrained (McKain et al. (4) found NG emissions to be 3X higher than the prior estimate), so the C_2H_6:CH_4 ratio allows us to better match the proportion of emissions from each source. This is important because of the different spatial distribution of different source sectors, with biological CH_4 sources (landfills, wetlands) located farther from the city, and NG CH_4 sources more concentrated in urban areas. Total NG emissions were scaled such that they contributed on average 91%, 84%, and 76% of the model ΔCH_4 (=prior*footprint) at the urban sites in the dormant, transitional, and growing seasons, respectively. We calculated a multiplier for each 2-month period (Jan/Feb, Dec/Mar, Nov/Apr, May/Oct, Jun/Sep, Jul/Aug) which, when multiplied by the NG portion of the prior inventory, made the NG component of the model ΔCH_4 equal to the fraction of CH_4 from NG. This footprint-weighted approach was used because the Boston sites where C_2H_6 and CH_4 were measured are not equally sensitive to emissions from across the study region – they are more sensitive to nearby sources, and the C_2H_6:CH_4 ratio reflects emissions in the footprint of the site, which is more influenced by urban than rural sources. Therefore, while we found the NG component of CH_4 to be 76%-91% in the footprint of the urban sites, after scaling emissions to match the NG fraction in the footprint, we calculate NG fractions of 32% in summer and 59% in winter across the entire 90-km radius circle study domain. Across the urban region, a 45-km radius circle around Boston, NG contributes 46% of total CH4 in the summer and 76% in the winter. For the purposes of comparing top-down with bottom-up emissions, we used the original NG emissions inventory, without any scaling to the ethane:methane ratio.

S3. Ethane-Methane Ratio Analysis

Ethane concentrations were measured using a laser spectrometer (16) at BU for 3 months in the fall and winter of 2012-13 and 1 month in the late spring of 2014 (4); they were measured via aircraft in August/September 2017 and March 2018 (17); they were also measured at COP for 5 months in the fall and winter of 2019-2020. The analysis of the observations from 2012-2014 has been previously described in (4). Following that method, to quantify the relationship between atmospheric C_2H_6 and CH4, we used χ^2 minimization (equation below) of a straight-line fit (b=slope, a=intercept) to 5-minute medians of 1 Hz data points (Figure S1), with errors in each variable characterized by the standard error of the mean (σ).

$$\chi^2(a,b) = \sum_{i=1}^{N} \frac{(y_i - a - bx_i)^2}{\sigma_{yi}^2 + b^2\sigma_{xi}^2}$$

5-minute medians were used to eliminate any potential influence of building emissions. We calculated a slope separately on each day with correlation between the two species of R^2>0.75. Because C_2H_6 measurements were not available at the background stations, the framework assumes that background concentrations did not vary substantially during individual days, supported by the tight correlation (R^2>0.75) between observed C_2H_6 and CH_4 on approximately half of the days. Days that did not have consistent C_2H_6:CH_4 ratios, typically because of changes in wind direction and therefore the source types in the measurement footprint, were not used in the analysis. Note in Figure S1 that there is a fairly large range of C_2H_6:CH_4 slopes, even though the R^2 between the 2 species shows very tight correlations on individual days. This is indicative of a different mix of biological vs. NG sources in the measurement footprint on days with different wind directions.

Three major pipelines, Tennessee (TGP), Algonquin (ALG) and Maritimes and Northeast (MNE), and a liquefied natural gas (LNG) import terminal supply NG to the Boston region. During the 2019-2020 measurement period, the three pipelines delivered the following fractions of NG consumed in Massachusetts: 61% TGP, 33% ALG, and 6% MNE (18). Hourly C_2H_6:CH_4 ratios in supplied NG were collected for each pipeline using hourly gas quality data from the measurement stations closest to Boston (Figure S2) REFS. Seasonal average C_2H_6:CH_4 ratios for the measurement period were calculated by averaging daily median C_2H_6 and CH_4 fractions for each pipeline. The ratios from the three pipelines were then weighted by their fractional contribution to consumption in MA, to yield a pipeline average ratio of 2.1%. Comparing this to the average ratio from the slope of observed C_2H_6:CH_4 of 1.85%, yields 88% of CH_4 originating from NG.

Gas composition in the pipelines is measured using industry standard methods (19) (20), but uncertainties due to sampling and measurement error are not reported. Additionally, the representativeness of the measured relative to the lost gas is not known. The approach described above to estimate the mean pipeline C_2H_6 and CH_4 ratio is intended to yield an aggregate estimate that is robust to sporadic erroneous and/or unrepresentative measurements.

S4. Optimized CH_4 and NG emissions

Figure 5 compares optimized NG emissions and total methane emissions with state-level residential and commercial NG consumption for MA. Figure S5 shows the same comparison for the BU site. As the COP site has a larger footprint than the BU site, we expect state-level consumption values to be more representative of consumption in its footprint than in the BU footprint (city-level NG consumption was not available). Thus, it is unsurprising that the correlation between emissions derived from BU measurements and state-level consumption is weaker. Total CH_4 and NG emissions derived from each site are similar, but with a larger seasonal amplitude at the COP site. Comparing the NG loss rate to residential and commercial consumption (Figure S6) also demonstrated this difference between the two sites. At the COP site, a constant loss rate is observed regardless of season, whereas at the BU site the increase in winter emissions is smaller than the increase in consumption, leading to lower loss rates in the winter. However, state-level consumption is not necessarily representative of consumption in the footprint of the BU site. It is possible that the NG emissions sources in the footprint of the BU site have less seasonal variability than those in the footprint of the COP site, and comparison to more relevant local consumption would produce a different relationship. We therefore focus on the COP results when comparing NG emissions with consumption in this study, as the footprint of the 215 m site is more relevant to state-level data.

S5. Inverse Model Sensitivity Studies

We tested a range of NG and wetland emissions in our prior inventory to assess their impact on optimized emissions calculated with our model. Due to large uncertainties in prior NG emissions estimates, rather than using the total NG emissions estimated in our prior inventory, we kept the spatial distribution of emissions, but scaled the NG emissions to be consistent with the attribution results from ethane data. In the main model configuration, the prior NG emissions were scaled such that they contributed on average 91%, 84%, and 76% of the footprint-weighted ΔCH_4 at the urban sites in the dormant, transitional, and growing seasons, respectively. These percentages are based on the average of measurements taken in from the BU site in 2012-2013 (3), an aircraft campaign in 2017-2018 (17), and from the COP site in 2019-2020 (Table 1). To test the impact of uncertainty in the fraction of methane from NG sources, particularly because the ethane measurements were not continuous during the study period, we ran the model with NG fractions spanning the range of measurements from the studies. We also tested using the unscaled NG emissions from the prior inventory (Table S2).

In addition, we tested a range of prior wetland emissions because estimates of emissions from different sources vary significantly. McKain et al. (3) estimated average wetland CH_4 emissions within our study area to be 0.67 $Mg/km^2/y$ (the inventory had no seasonal variability in wetland emissions), while WetCHARTs estimates average emissions ranging from 1.3 – 9.8 $Mg/km^2/y$ depending on season. Because they tend to be located farther from our urban sites than the NG emissions, wetland emissions lead to relatively small changes in concentration at the receptor, so even large differences in prior estimates are not expected to significantly change the modeled enhancement at the urban sites. We used sensitivity studies to quantify the impact of the range of possible wetland emissions. We tested wetland emissions from McKain (seasonally-invariant), and from WetCHARTs, maintaining their seasonal variability. We also tested ½ and ¼ of WetCHARTs emissions, maintaining their seasonal variability, as midpoints between the WetCHARTs and McKain inventories. All permutations studied are shown in Table S2.

Seasonal average CH_4 and NG emissions from the sensitivity studies are shown in Figure S7. The minimum and maximum NG emissions from the 11 configurations are shown as dashed lines and the gray shaded region is the range from the 25^{th}-75^{th} percentile of emissions in each season. The different configurations lead to a much larger range of CH_4 emissions than NG emissions, with CH_4 emissions typically within ±20% of the main configuration, and one configuration (#10, which had no seasonal variability in the NG or wetland emissions prior) ~35% lower emissions than the main configuration in the summer. NG emissions, on the other hand, are always within ±20% of the main configuration and typically within ±15%. We tested prior wetland emissions which ranged by over a factor of 14; these scenarios produced posterior wetland emissions which ranged by a factor of 3.5. However, because wetlands tend to be located significantly farther from the urban receptors than NG sources, they do not have a substantial impact on the enhancement at the receptor. This uncertainty in posterior wetland emissions therefore did not translate to significant uncertainty in optimized NG emissions. Therefore, our network cannot strongly constrain emissions from biological sources, leading to higher uncertainty in total methane emissions in the summer (Figure S7). However, we do have confidence in the NG component of methane emissions throughout the year, as these emissions are concentrated near the receptors.

We also investigated whether days easterly winds could be used to shed light on wetland methane emissions. We found that the wetland methane source in our prior inventory is not

significantly different for east vs. west winds. The urbanized area near Boston does not have significant wetlands along the coast; there are some wetlands along the coast to the north and south of Boston and on Cape Cod, but there are also substantial wetlands to the west of Boston. Over the 7 summers in our dataset (when wetland emissions are the highest), on days when MA was used as a background site, on average 17% of the total model CH_4 enhancement came from wetland emissions. For days with HF or CA backgrounds, 17% of the total enhancement came from wetlands as well. For east angles (30 – 120°), only 6% of the total CH_4 enhancement was from wetland emissions. Thus, we were not able to use wind direction to separate biogenic and anthropogenic methane sources in the Boston area.

We tested the impact of excluding east winds (0-120°) from our analysis by running the model using those angles with MA as a background. We found no difference in model results - total CH_4 and NG emissions from this run agreed with our main configuration to within 2%.

S6. Atmospheric CH_4 enhancement over time

We saw no trend in ΔCH_4 between our Boston and background sites over the study time period (Figure S3). April, 2020, stands out in the time series (red dot) as the only month when the average enhancement at the 29 m BU site was lower than that at the 215 m COP site, indicating a significant change in concentration at the BU site.

S7. NG consumption during COVID-19 shutdown.

Massachusetts total NG consumption during April 2020 showed no change in the residential, commercial, or industrial sectors compared to previous years, while the electrical sector showed a 35% decrease in consumption compared to 2018 and 2019 (21) (Figure S8).

S8. Multi-city comparison

Three studies in Los Angeles have calculated top-down methane emissions over 4-8 years (22) (23) (24); all were remote sensors which employed a tracer:tracer method tied to prior inventories of CO_2 or CO, with the assumption that emissions of CH_4 are co-located with the other species. Only Wunch et al. (22) determined the fraction of methane due to NG, and only He et al. (23) calculated the consumption of NG in the measurement footprint. The longest previous studies which use atmospheric measurements with prior CH_4 inventories to derive emissions are for 2 and 3 years from Los Angeles (25) and Indianapolis (26), respectively.

Figure 7 compares this study's top-down and bottom-up NG emissions for Boston with other cities that have been studied across the US. In order to compare NG emissions from as many studies as possible, we calculated the NG emissions for top-down studies which estimated total methane emissions only by multiplying methane emissions by the fraction of methane from NG determined by other studies of the same city. Aircraft-based CH_4 emissions from Balashov et al. (26) in Indianapolis were multiplied by 43%, the NG calculated by Lamb et al. (27), to calculate NG emissions. Methane emissions in Los Angeles from Yadav et al. (25), Cui et al. (28), and Wong et al. (24) were all multiplied by 58%, the NG fraction from Wunch et al. (22) to calculate NG emissions. Methane emissions in the Washington D.C./Baltimore metro area from Huang et al. (29), were multiplied by 67.5%, the average of the NG fractions calculated by Ren et al. (30) and Plant et al. (31).

Among these studies, loss rates from NG infrastructure were calculated in different ways; for comparison, we re-calculated loss rates for some studies according to our method (Table S3). In Washington D.C., Ren et al. (30) calculated loss rates from NG distribution and end use of

1.1% and 2.1% during flights in winter 2015 and 2016, respectively (using a method similar to ours). Huang et al. (29) used 4 months of tower measurements from Washington D.C. from different seasons to estimate a loss rate of 1.3% by assuming that the seasonally varying component of methane emissions was due to NG loss. However, this assumes that none of the seasonally invariant methane emissions are due to NG, which is likely not the case for pipeline emissions, and does not account for seasonal variability in biological CH_4 emissions. We re-computed the loss rate by multiplying CH_4 emissions from Huang et al. with the fractional contribution of NG to CH_4 emissions estimated by Ren et al. and Plant et al. (31) and comparing to NG consumption, and found loss rates of 1.1% and 2.1%, respectively. In Los Angeles, He et al. (23) calculated a loss rate of 1.3% from end use only (not including pipeline mains and transmission) based on the seasonal variability of methane emissions. We computed a loss rate for all distribution and end use by multiplying CH_4 emissions by the fractional contribution of NG to CH_4 emissions estimated by Wunch et al. (22), and calculated a total loss rate of 2.3%. Peischl et al. also estimated the loss rate for Los Angeles based on aircraft measurements to be 2% of consumed NG.

To estimate how NG losses from distribution and end use compare to losses from the entire US NG supply chain, we used estimates of supply chain losses from Saint Vincent et al. (32). Saint Vincent calculate that U.S. losses from NG distribution and end use constitute 6% of losses from the natural gas supply chain. Our analysis for Boston and review of studies from other cities indicate that top-down emissions are 3-6 times larger than the bottom-up studies used in the Saint Vincent et al. estimate (Saint Vincent did not have access to all of the recent studies in our updated inventories, and their bottom-up estimates were lower than current estimates). If the emissions from these cities are representative of emissions across the country, scaling the distribution and end use component from Saint Vincent et al. by 3-6 fold leads to NG losses from distribution and end use amounting to 20-36% of all losses from the NG supply chain, and 6-11% of all anthropogenic methane emissions (including agriculture).

S9. Massachusetts pipeline leaks and repairs

The city of Boston has set a goal of becoming carbon neutral by 2050 (34), and Massachusetts implemented new laws and regulations between 2014 and 2019 requiring utilities to report and repair large leaks based on their size (35) (36). A 2014 law required repair of leaks classified as grade 1 and grade 2, as well as making leak data public. A 2018 law required repair of grade 3 leaks classified as "significant environmental impact" as well. Figure S9 shows the leak counts and leaks repaired each year since 2014. Unfortunately, data is not available before the 2014 law took effect to judge the impact of the 2014 law. However, our top-down model does go back to mid-2012 and should see any changes from these laws. In the gas company data going back to 2014, there was no significant change in the number of grade 1 or 2 leaks on the pipeline system, and only a slight reduction in the number of grade 3 leaks, with no sign of change after the 2018 law (37). This data shows that the gas companies are replacing 4-5% of leak-prone pipe each year, with a lot of leak-prone pipe remaining in the system. In the aging Boston pipeline system, new leaks are appearing as fast as old ones are being fixed. While there was hope that these policies would significantly reduce the methane emissions from distribution pipelines, neither our top-down analysis of emissions nor counts of leaks on the system have shown a decrease.

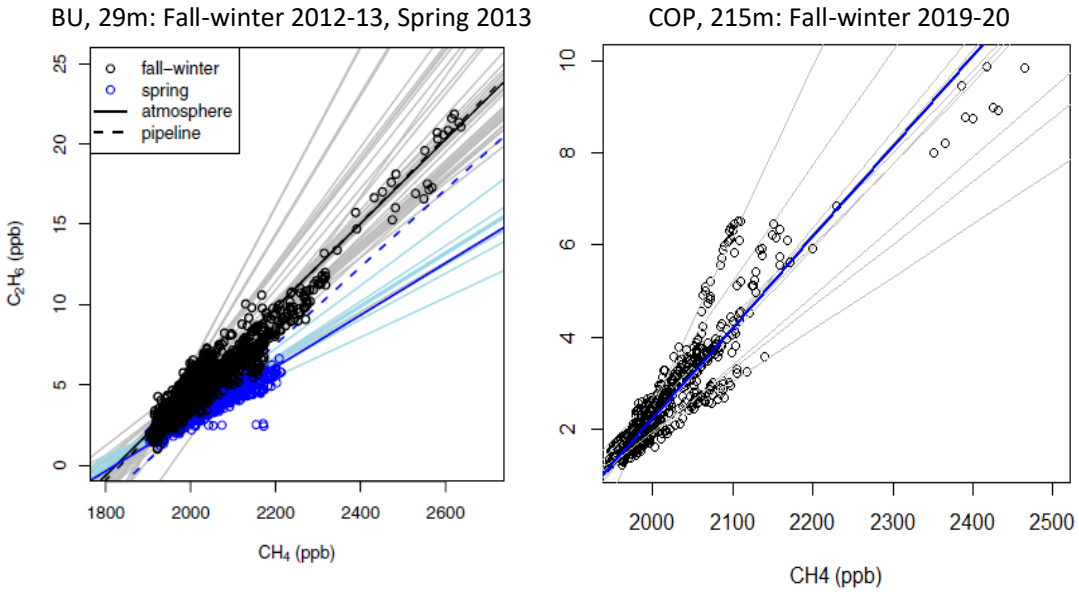

Figure S1: Five-minute median atmospheric C_2H_6 vs. CH_4 measurements. Left: From McKain et al. (4), measurements at BU in fall and winter of 2012-2013 (black) and spring of 2014 (blue). χ^2 optimization lines fit to each day (light lines) and average fit lines for both seasons from all days with $R^2>0.75$ (bold lines), and lines with slopes of pipeline C_2H_6/CH_4 (dashed line). Right: Same, but for measurements at COP in fall-winter 2019-2020.

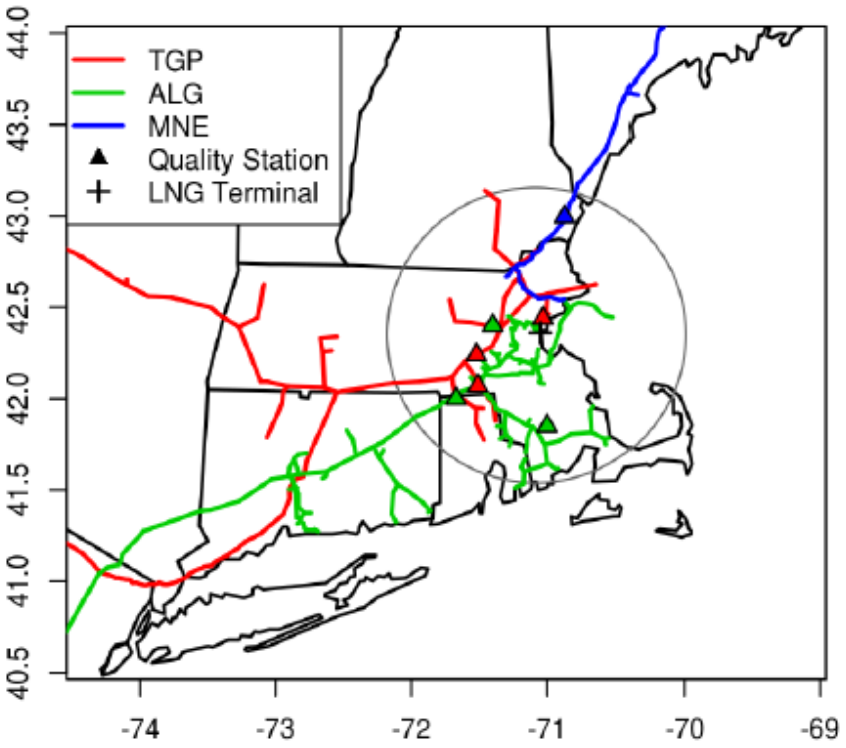

Figure S2: From McKain et al. (3). Approximate locations of the three interstate gas pipelines (Tennessee- TGP, Algonquin (ALG), and Maritimes and Northeaset (MNE) serving Boston and the surrounding area, the gas quality measurement stations used in this study, and the LNG import terminal. The gray circle is the study boundary.

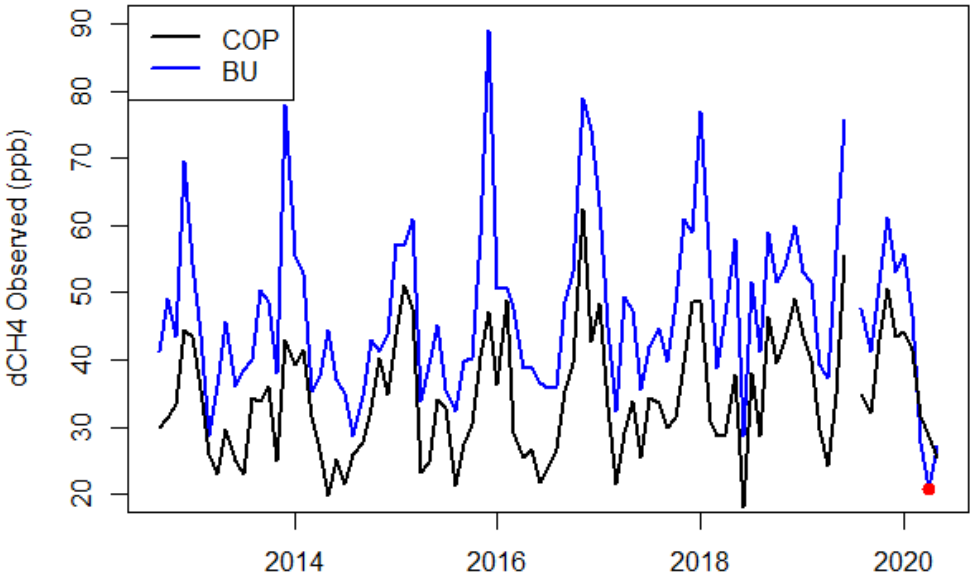

Figure S3: Time series of monthly average ΔCH_4 between our urban sites (COP/BU) and our background concentrations. Red point indicates April 2020.

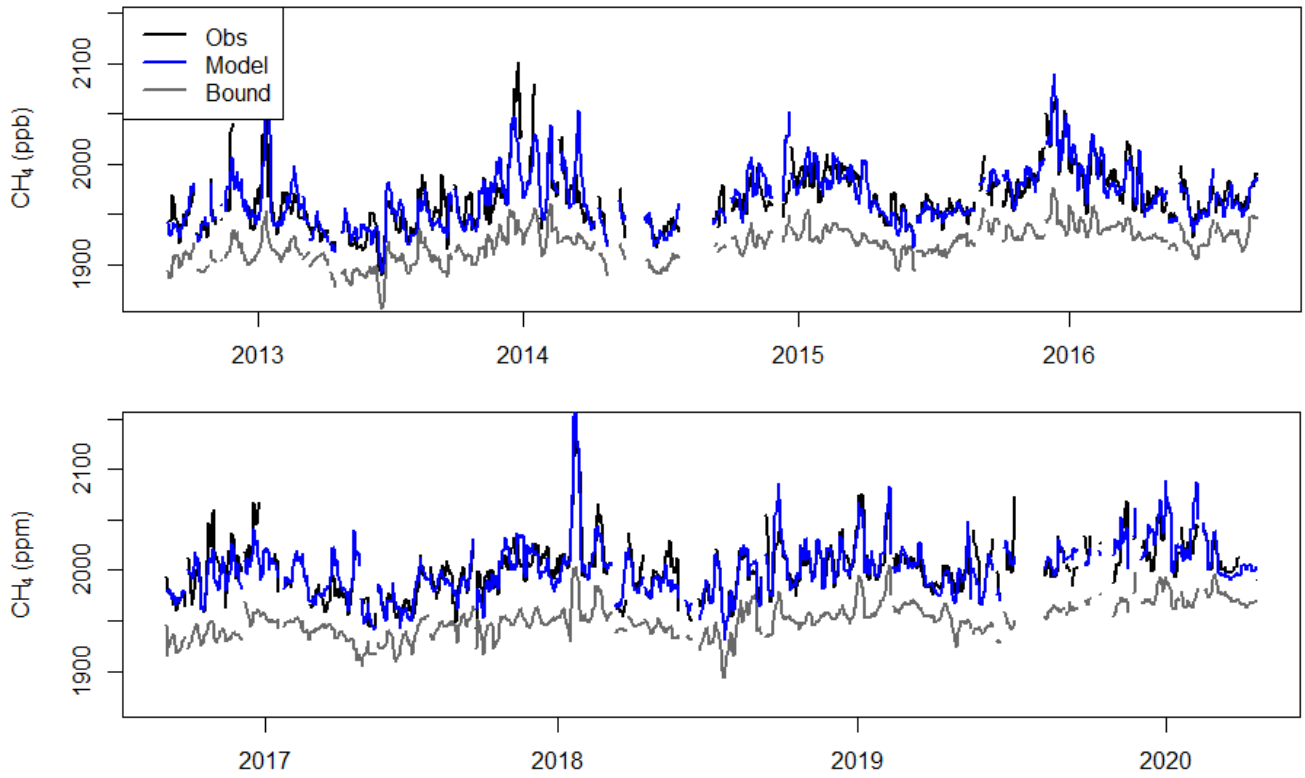

Figure S4: Observed (Obs), scaled model (Model), and boundary (Bound) CH_4 at COP. Seven-day running afternoon average for the entire study period.

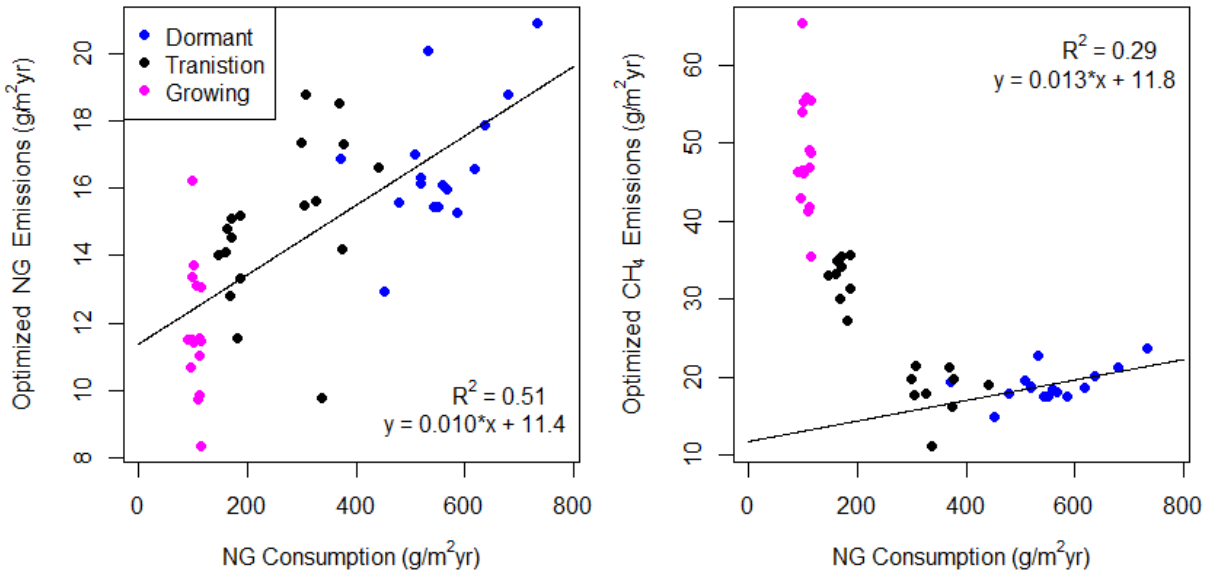

Figure S5: Optimized NG emissions (left) and total methane emissions (right) compared to residential and commercial NG consumption in MA based on measurements at the BU site. Linear fit to all data (left) and dormant season data (Dec. – Mar.) (right) is shown. Each point represents a two-month average.

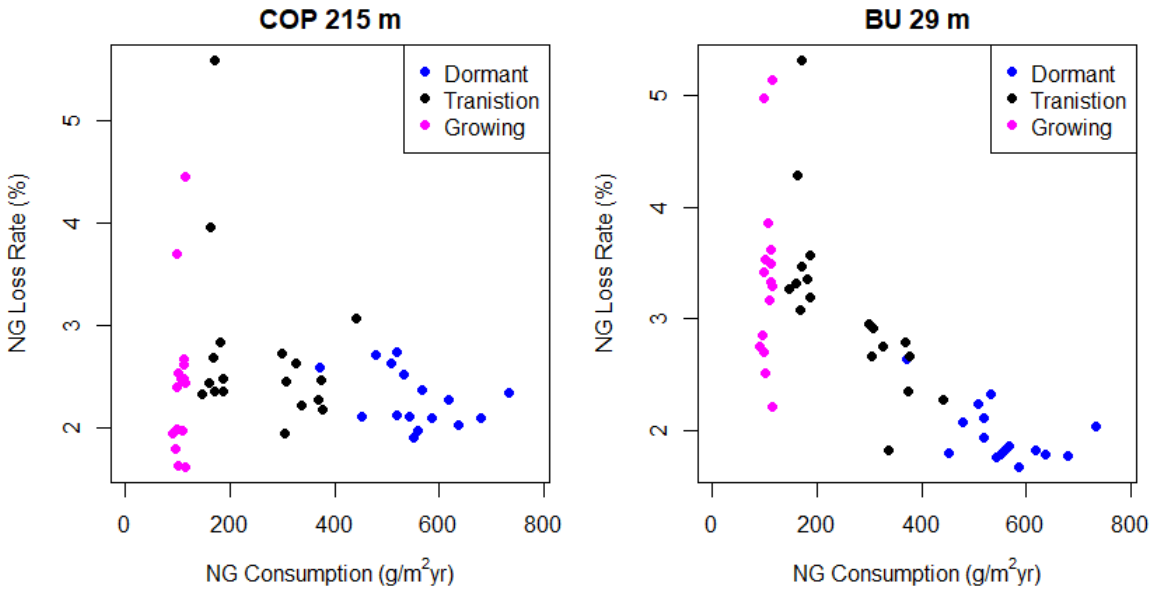

Figure S6: NG loss rate derived from observations at our COP (left) and BU (right) sites compared to MA NG consumption.

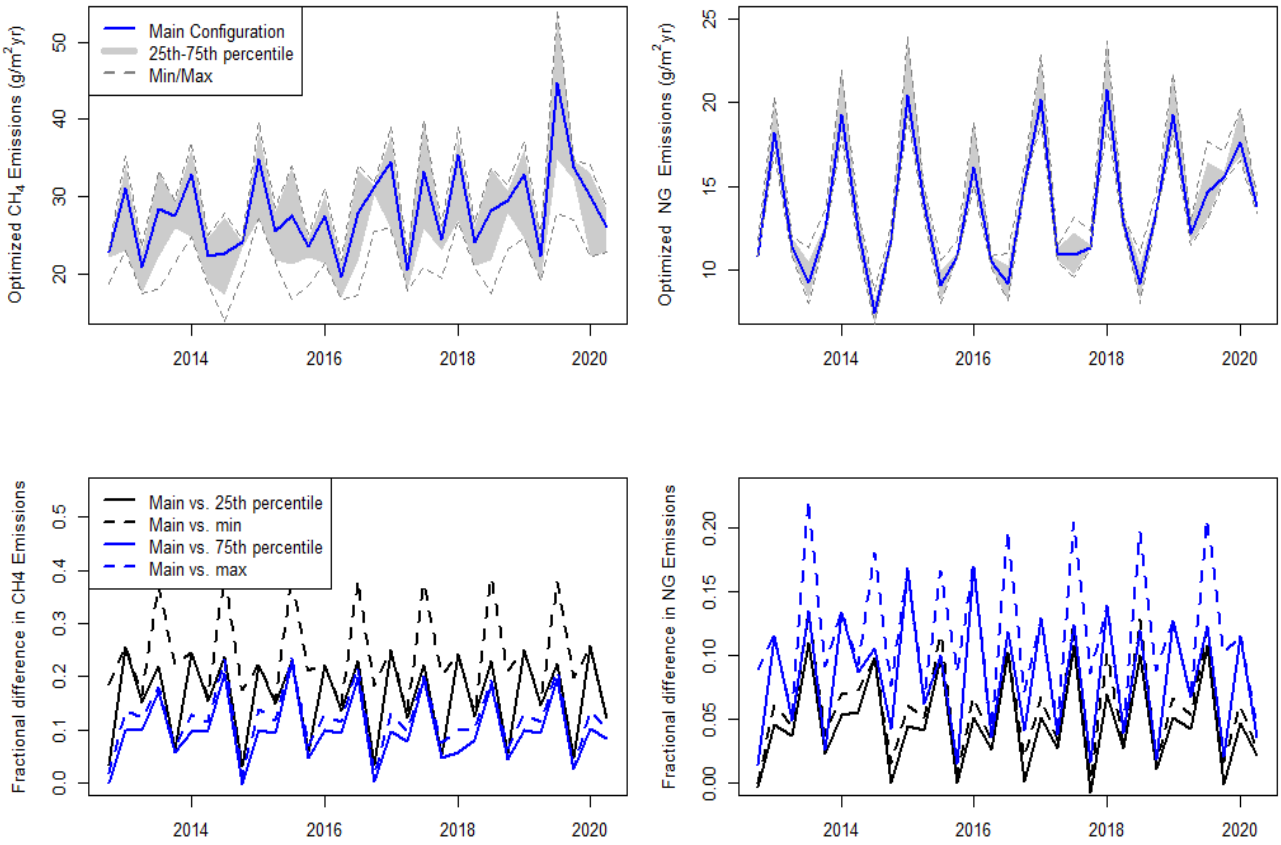

Figure S7: Top left: Seasonal average optimized CH_4 emissions based on the COP site from the 11 configurations in Table S2. Shown are the main configuration presented in the paper (blue) and maximum and minimum emissions from the 11 configurations (gray dashed). The 25^{th}-75^{th} percentile of the 11 configurations fall in the gray shaded area. Top right: Same, but for NG emissions. Bottom left: Fractional difference between CH_4 emissions calculated with our main configuration and the minimum, maximum, 25^{th}, and 75^{th} percentile of those calculated using the 11 configurations. Bottom right: Same, but for NG emissions. Ticks on x-axis represent January of each year.

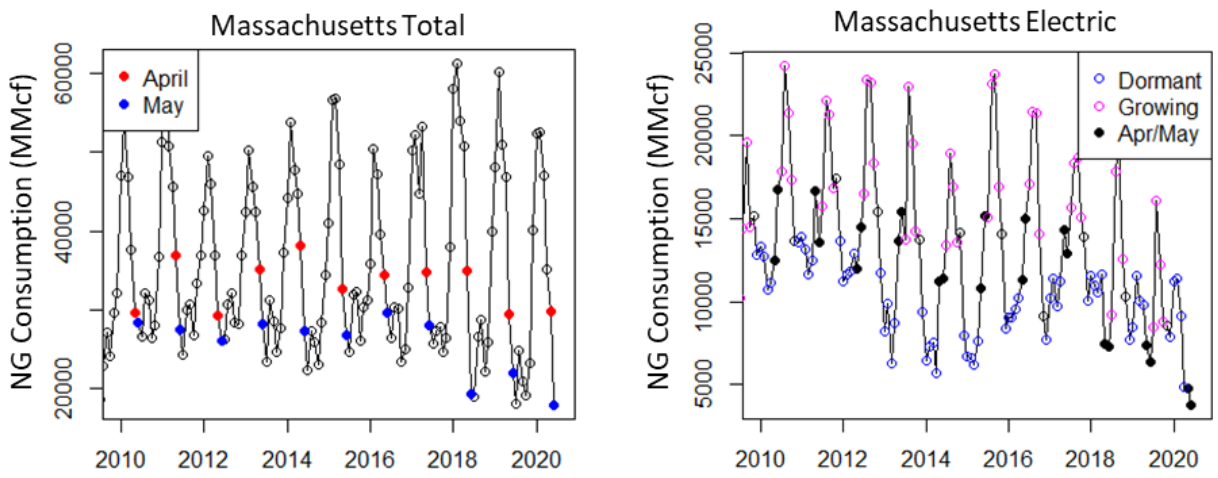

Figure S8: Left: Massachusetts total NG consumption during the study period. April data is shown in red and May in blue for better comparison of the COVID-19 shutdown period with previous years. Right: Massachusetts electrical sector NG consumption during the study period. April and May data are shown as black dots.

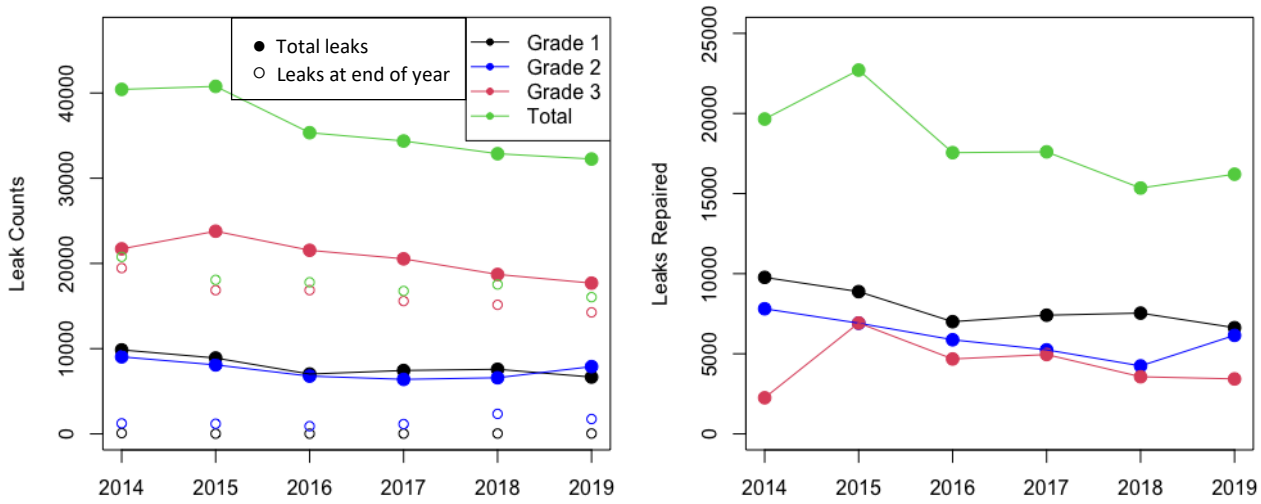

Figure S9: Left: Leak counts from all Massachusetts natural gas companies per year for Grade 1, Grade 2, Grade 3, and total leaks (37). Filled circles represent leaks on the system at any time during the calendar year; open circles represents leaks remaining on the system at the end of the year. Right: Leaks repaired per year by grade.

Table S1. Summary of Boston urban greenhouse gas network

Site	Operator	Abbrev.	Latitude	Longitude	Elevation (m)	Sampling Height (m)
Copley Square	Harvard	COP	42.35	70.08	6	215
Boston Univ.	Harvard/BU	BU	42.35	71.10	4	29
Harvard Forest	Harvard	HF	42.54	72.17	340	29
Canaan, NH	ENI	CA	43.71	72.15	559	100
Mashpee, MA	ENI	MA	41.66	70.50	32	46

Table S2. NG and wetland emissions configurations used in sensitivity studies to assess their impact on optimized model emissions. NG%: Percentage of CH_4 emissions from the NG sector in the prior inventory in the dormant/transitional/growing seasons. Wetland emission totals were based on WETCHARTS (9) or McKain et al. (3), or a fraction of the WETCHARTS total.

	NG %	Wetlands
Main	91/84/76	½ WetCHARTs
1	98/83/67	WetCHARTs
2	98/83/67	½ WetCHARTs
3	98/83/67	¼ WetCHARTs
4	98/83/67	McKain
5	87/86/85	WetCHARTs
6	87/86/85	½ WetCHARTs
7	87/86/85	¼ WetCHARTs
8	87/86/85	McKain
9	Unscaled	½ WetCHARTs
10	Unscaled	McKain

Table S3. NG losses as a percent of the NG consumed in the study area, showing loss rates published in the original study as well as calculated according to our methodology.

Study	City	Published NG Loss Rate	Re-calculated NG Loss Rate
Ren et al. (30)	Washington D.C.	1.1% / 2.1%[a]	
Huang et al. (29)	Washington D.C.	1.3%	1.1% / 2.1%[b]
He et al. (23)	Los Angeles	1.3%	2.3%
Peischl et al.	Los Angeles	2%	
McKain et al.	Boston	2.7%	
This study	Boston	2.5%	

a) 1.1% during winter 2015, 2.1% during winter 2016
b) 1.1% based on NG fraction from Ren et al., 2.1% based on NG fraction from Plant et al.

SI References

1. A cavity ring-down analyzer for measuring atmospheric levels of methane, carbon dioxide, and water vapor. Crosson, E. R. 2008, Appl Phys B, pp. 92(3), 403–408.
2. Rella CW, et al. (2013) High-accuracy measurements of dry mole fractions of carbon dioxide and methane in humid air. Atmos Meas Tech 6: 837-860.
3. McKain K, et al. (2015) Methane emissions from natural gas infrastructure and use in the urban region of Boston, Massachusetts. Proc Natl Acad Sci U.S.A. 112(7):1941-6.
4. K. McKain et al., Methane emissions from natural gas infrastructure and use in the urban region of Boston, Massachusetts, Proc. Nat. Acad. Sci., 112, 1941-1946 (2015) 2015.
5. U.S. Environmental Protection Agency (2019) 2018 Greenhouse Gas Emissions from Large Facilities, http://ghgdata.epa.gov/ghgp.
6. Massachusetts Department of Environmental Protection, Active Landfills, https://www.mass.gov/doc/list-of-active-landfills-in-massachusetts-january-2020/download.
7. Massachusetts Department of Environmental Protection, Inactive and Closed Landiflls, https://www.mass.gov/doc/list-of-inactiveclosed-landfills-dumping-grounds-in-massachusetts-january-2020/download.
8. Landfill Methane Outreach Program (LMOP), Project and Landfill Data by State, https://www.epa.gov/lmop/project-and-landfill-data-state.
9. Bloom, A.A. et al., 2017. CMS: Global 0.5-deg Wetland Methane Emissions and Uncertainty (WetCHARTs v1.0). ORNL DAAC, Oak Ridge, Tennessee, USA. https://doi.org/10.3334/ORNLDAAC/1502.
10. M. L. Fischer et al., An estimate of natural gas methane emissions from California homes, Environ. Sci. Technol., 52, 10205−10213 (2018).
11. Z. Merrin, P. W. Francisco, Unburned methane emissions from residential natural gas appliances, Environ. Sci. Technol., 53, 5473−5482 (2019).
12. E. D. Lebel, H. S. Lu, S. A. Speizer, C. J. Finnegan, R. B. Jackson, Quantifying methane emissions from natural gas water heaters, Environ. Sci. Technol., 54, 9, 5737–5745 (2020).
13. Califofornia Energy Commission, Characterization of Fugitive Methane Emissions from Commercial Buildings in California.
14. Z. D. Weller, S. P. Hamburg, J. C. von Fischer, A national estimate of methane leakage from pipeline mains in natural gas local distribution systems, Environ. Sci. Technol., 54 (14), 8958-8967 (2020).
15. Greenhouse Gas Baseline, Inventory & Projection, Appendix C: Massachusetts Annual Greenhouse Gas Emissions Inventory: 1990-2017, with Partial 2018 & 2019 Data, https://www.mass.gov/lists/massdep-emissions-inventories.
16. Yacovitch TI, et al. (2014) Demonstration of an ethane spectrometer for methane source identification. Environ Sci Technol 48(14):8028–8034.
17. C. Floerchinger et al., Relative flux measurements of biogenic and natural gas-derived methane for seven U.S. cities. Elementa: Science of the Anthropocene, (1): 000119 (2021).
18. U.S. EIA, Natural Gas Annual Respondent Query System. Receipts from State or US Boarder Volume. https://www.eia.gov/naturalgas/ngqs/#?year1=2015&year2=2018&company=Name.
19. Gas Processing Association (2013) Analysis for natural gas and similar gaseous mixtures by gas.

20. ASTM International (2010) Standard test method for analysis of natural gas by gas chromatography,.
21. EIA https://www.eia.gov/dnav/ng/ng_cons_sum_dcu_nus_m.htm.
22. D. Wunch et al., Quantifying the loss of processed natural gas within California's South Coast Air Basin using long-term measurements of ethane and methane, Atmos. Chem. Phys., 16, 14091–14105 (2016).
23. L. He et al., Atmospheric methane emissions correlate with natural gas consumption from residential and commercial sectors in Los Angeles, Geophys. Res. Lett., 46, 8563–8571 (2019).
24. C. K. Wong et al., Monthly trends of methane emission in Los Angeles form 2011 to 2015 inferred by CLARS-FTS observations, Atmos. Chem. Phys., 16, 13121–13130 (2016).
25. V. Yadav et al., Spatio-temporally resolved methane fluxes from the Los Angeles megacity, J. Geophys. Res.: Atm., 124, 5131–5148 (2019).
26. N. V. Balashov et al., Background heterogeneity and other uncertainties in estimating urban methane flux: results from the Indianapolis Flux Experiment (INFLUX), Atmos. Chem. Phys., 20, 4545–4559 (2020).
27. B. K. Lamb et al, Direct and indirect measurements and modeling of methane emissions in Indianpolis, Indiana, Environ. Sci. Technol., 50, 8910−8917 (2016).
28. Y.Y. Cui et al., Top-down estimate of methane emissions in California using a mesoscale inverse modeling technique: The South Coast Air Basin, J. Geophys. Res. Atmos., 120, 6698–6711 (2015).
29. Y. Huang et al, Seasonally resolved excess urban methane emissions from the Baltimore/Washington, DC metropolitan region, Environ. Sci. Technol., 53, 11285−11293 (2019).
30. X. Ren et al., Methane emissions from the Baltimore-Washington area based on airborne observations: Comparison to emissions inventories, J. Geophys. Res. Atm., 123, 8869–8882 (2018).
31. G. Plant, E. C. Kort, C. Floerchinger, A. Gvakharia, I. Vimont, C. Sweeney, Large fugitive methane emissions from uban centers along the U.S. east coast, Geophys. Res. Lett., 46, 8500–8507 (2019).
32. P. M. B. Saint-Vincent, N. J. Pekney, Beyone-the-Meter: Unaccounted sources of methane emissions in the natural gas distribution sector, Environ. Sci. Technol., 54, 39−49 (2020).
33. J. Peischl et al., Quantifying sources of methane using light alkanes in the Los Angeles basin, California, J. Geophys. Res. Atmos., 118, 4974–4990, doi:10.1002/jgrd.50413 (2013).
34. City of Boston (2017) Climate Action Plan (City of Boston, Boston, MA). https://www.boston.gov/departments/environment/climate-action-plan. Accessed June 11, 2021.
35. B. Moran (April 1, 2019), New State Regulation Could Cut Emissions From Natural Gas Leaks In Half, Report Says. https://www.wbur.org/earthwhile/2019/04/01/natural-gas-methane-leaks-massachusetts-rule. Accessed 7/15/21.
36. Gas Leak Allies, Laws and Regulations. https://www.gasleaksallies.org/laws-and-regulations. Accessed 7/15/21.
37. Report on the Prevalence of Natural Gas Leaks in the Natural Gas System to the Joint Committee on Telecommunications, Utilities, and Energy, and the Joint Committee on Public Safety and Homeland Security, pursuant to An Act Relative to Natural Gas Leaks, St. 2014, c. 149, § 9. https://eeaonline.eea.state.ma.us/DPU/Fileroom/dockets/bynumber, accessed 7/15/2021. Search for 20-GLR-01, 19-GLR-01, … 15-GLR-01. Accessed 7/12/21.